



HAL
open science

Drought-induced lacuna formation in the stem causes hydraulic conductance to decline before xylem embolism in Selaginella

Amanda A Cardoso, Dominik Visel, Cade N. Kane, Timothy Batz, Clara Garcia Sàncchez, Lucian Kaack, Laurent Lamarque, Yael Wagner, Andrew King, Jose Manuel Torres Ruiz, et al.

► To cite this version:

Amanda A Cardoso, Dominik Visel, Cade N. Kane, Timothy Batz, Clara Garcia Sàncchez, et al.. Drought-induced lacuna formation in the stem causes hydraulic conductance to decline before xylem embolism in Selaginella. *New Phytologist*, 2020, 227 (6), pp.1804-1817. 10.1111/nph.16649 . hal-02927433

HAL Id: hal-02927433








<https://hal.inrae.fr/hal-02927433v1>

Submitted on 1 Sep 2020

HAL is a multi-disciplinary open access archive for the deposit and dissemination of scientific research documents, whether they are published or not. The documents may come from teaching and research institutions in France or abroad, or from public or private research centers.

L'archive ouverte pluridisciplinaire **HAL**, est destinée au dépôt et à la diffusion de documents scientifiques de niveau recherche, publiés ou non, émanant des établissements d'enseignement et de recherche français ou étrangers, des laboratoires publics ou privés.

Drought-induced lacuna formation in the stem causes hydraulic conductance to decline before xylem embolism in *Selaginella*

Amanda A. Cardoso¹ , Dominik Visel², Cade N. Kane¹, Timothy A. Batz¹, Clara García Sánchez², Lucian Kaack², Laurent J. Lamarque³, Yael Wagner⁴, Andrew King⁵, José M. Torres-Ruiz⁶ , Déborah Corso³ , Régis Burlett³, Eric Badel⁶, Hervé Cochard⁶ , Sylvain Delzon³ , Steven Jansen²  and Scott A. M. McAdam¹ 

¹Purdue Center for Plant Biology, Department of Botany and Plant Pathology, Purdue University, West Lafayette, IN 47907, USA; ²Institute of Systematic Botany and Ecology, Ulm University, Albert-Einstein-Allee 11, Ulm 89081, Germany; ³INRAE, BIOGECO, University of Bordeaux, Pessac 33615, France; ⁴Department of Plant & Environmental Sciences, Weizmann Institute of Science, Rehovot 76100, Israel; ⁵Synchrotron Source Optimisée de Lumière d'Énergie Intermédiaire du LURE, L'Orme de Merisiers, Saint Aubin-BP48, Gif-sur-Yvette Cedex, France; ⁶INRAE, PIAF, Université Clermont-Auvergne, Clermont-Ferrand 63000, France

Summary

Author for correspondence:
Scott A. M. McAdam
Tel: +1 765 494 3650
Email: smcadam@purdue.edu

Received: 18 March 2020
Accepted: 22 April 2020

New Phytologist (2020)
doi: 10.1111/nph.16649

Key words: ABA, embolism, evolution, hydraulic conductance, lycophyte, stomatal conductance, stomatal evolution.

- Lycophytes are the earliest diverging extant lineage of vascular plants, sister to all other vascular plants. Given that most species are adapted to ever-wet environments, it has been hypothesized that lycophytes, and by extension the common ancestor of all vascular plants, have few adaptations to drought.
- We investigated the responses to drought of key fitness-related traits such as stomatal regulation, shoot hydraulic conductance (K_{shoot}) and stem xylem embolism resistance in *Selaginella haematodes* and *S. pulcherrima*, both native to tropical understory.
- During drought stomata in both species were found to close before declines in K_{shoot} , with a 50% loss of K_{shoot} occurring at -1.7 and -2.5 MPa in *S. haematodes* and *S. pulcherrima*, respectively. Direct observational methods revealed that the xylem of both species was resistant to embolism formation, with 50% of embolized xylem area occurring at -3.0 and -4.6 MPa in *S. haematodes* and *S. pulcherrima*, respectively. X-ray microcomputed tomography images of stems revealed that the decline in K_{shoot} occurred with the formation of an air-filled lacuna, disconnecting the central vascular cylinder from the cortex.
- We propose that embolism-resistant xylem and large capacitance, provided by collapsing inner cortical cells, is essential for *Selaginella* survival during water deficit.

Introduction

Lycophytes, the earliest diverging, extant lineage of land plants to possess a vascular system, occupy a key phylogenetic position as sister to all other vascular plants (Ambrose, 2013). Lycophyte ancestors, or lycophyte-like plants, are found in the oldest fossil assemblages of land plants, and had probably diverged by the Late Silurian (Rowe, 1988; Klaus *et al.*, 2017). During the Carboniferous, lycophytes were the first group of land plants to evolve secondary growth and form the first trees that dominated equatorial swamp forests, comprising approximately half of floristic diversity at that time (Stewart & Rothwell, 2010). Lycophyte forests declined during a period of global aridification in the early Permian, with extant lycophytes represented by just three families: Lycopodiaceae (*c.* 390 spp.), the aquatic to semi-aquatic Isoetaceae (*c.* 250 spp.), and the most abundant and speciose family, Selaginellaceae (*c.* 700 spp.). *Selaginella*, the sole genus in Selaginellaceae, is the most ecologically diverse genus of lycophyte. While most species grow terrestrially in ever-wet temperate and tropical rainforest

understories, others grow as epiphytes, in alpine environments and deserts, where species are frequently desiccation-tolerant (Schneider *et al.*, 2004; Soni *et al.*, 2012; Pampurova & Van Dijck, 2014; Vanburen *et al.*, 2018).

Species of *Selaginella*, like all non-Isoetalean lycophytes, lack secondary growth. Their mature stems are usually flattened dorsoventrally, consisting of a cutinized epidermis, suberized hypodermis, cortex and a central vascular cylinder. The vascular cylinder or stele has centrally positioned xylem, surrounded by phloem, which is ultimately enclosed in a pericycle, generally composed of one layer of cells (Barclay, 1931; McLean & Juniper, 1979; Schulz *et al.*, 2010) (see Supporting Information Fig. S1). The inner cortex is often described as being separated from the vascular cylinder by an air-filled lacuna (Mickel & Hellwig, 1969; Buck & Lucansky, 1976). The cortex and pericycle are connected by trabeculae, highly modified, thin-walled endodermal cells which provide a symplastic connection through abundant plasmodesmata (McLean & Juniper, 1979; Schulz *et al.*, 2010). Trabeculae cells have a well-developed Casparian strip at the anticlinal cell walls, which may be additionally

covered with a thin layer of cutin forming the trabecular ring (McLean & Juniper, 1979). The presence of a Casparian strip has been demonstrated to efficiently restrict the transport of water-soluble compounds from the vascular tissue into the apoplast of cortical cells (Gola & Jernstedt, 2016). Water in the xylem must traverse the trabeculae to irrigate photosynthetic tissue.

The vascular system of *Selaginella* consists primarily of tracheids, while in some species vessels have been reported (Duerden, 1934; Schneider & Carlquist, 2000a,b). However, treatment with alcohol and various acids during sample preparation raises questions of whether shrunken and damaged pit membranes in the bordered pits of tracheids were misinterpreted as the perforation plates of vessels (Zhang *et al.*, 2017). Pit membranes are described as thin in tracheids and highly porous in the supposed vessels of *Selaginella* species (Schneider & Carlquist, 2000b), which given the importance of these structures for hydraulic efficiency and protection against embolism in angiosperms (Li *et al.*, 2016), could result in an efficient yet highly vulnerable water transport system (Brodersen *et al.*, 2014; Kaack *et al.*, 2019). Blockage to water flow in xylem cells by embolism at negative water potentials (Ψ) progressively reduces hydraulic conductance, limiting the transport of water within plants (Tyree & Sperry, 1989). Single air-seeding pressure measurements of xylem conduits of the desiccation-tolerant species *S. pallescens* suggest highly vulnerable xylem, with embolism first forming at -1.5 MPa (Brodersen *et al.*, 2014); this value matches the mean Ψ resulting in a 50% decline in shoot hydraulic conductance (K_{shoot}) in this species (Brodribb & Holbrook, 2004).

Given that extensive embolism is a primary cause of plant mortality during drought (Brodribb & Cochard, 2009; Urli *et al.*, 2013; Cardoso *et al.*, 2020), protecting the xylem from tensions that would induce embolism is of utmost importance for plant survival during prolonged drought. In seed plants, highly efficient stomatal closure is the primary means by which plants prevent declines in water status during soil water-limitation (Martin-StPaul *et al.*, 2017; Creek *et al.*, 2019). Species adapted to the most seasonally dry environments with xylem that embolizes before declining to -3 MPa, rely on stomatal closure driven by the hormone ABA to halt water loss during prolonged drought (Brodribb *et al.*, 2014). While stomatal closure is critical for reducing more than 95% of plant water loss during long-term drought (Franks & Farquhar, 2007), evaporation through the cuticle, and incompletely closed stomata, continues and ultimately drives declines in Ψ (Duursma *et al.*, 2018). In early diverging lineages of vascular land plants, including lycophytes and ferns, stomatal closure during changes in leaf water status, including periods of prolonged drought, is driven by passive reductions in guard cell turgor, and not metabolic mechanisms (Brodribb & McAdam, 2011; Deans *et al.*, 2017; Cardoso & McAdam, 2019; Cardoso *et al.*, 2019). Stomatal closure during drought in *S. pallescens* (Brodribb & Holbrook, 2004) and *S. kraussiana* (McAdam & Brodribb, 2013) occurs at the moderate Ψ of -1.2 MPa. This Ψ at complete stomatal closure slightly precedes the Ψ at which declines in K_{shoot} are

observed or when photosynthesis is irreparably damaged in both species (Brodribb & Holbrook, 2004; McAdam & Brodribb, 2013).

Other than the evolution of desiccation tolerance in *Selaginella* (Oliver *et al.*, 2000; Zhou *et al.*, 2016), results from the limited number of physiological studies, and constrained ecological preferences of this genus (Campany *et al.*, 2019), suggest that *Selaginella* species from wet environmental conditions do not possess adaptations to survive long periods of water deficit. We hypothesize that the xylem of tropical *Selaginella* species is highly vulnerable to embolism formation during drought. Furthermore, we expect that species from this genus have very few adaptations to tolerate water limitation, including a limited capacity to close stomata during drought. To address this, we examined the hydraulic vulnerability of shoots of two tropical *Selaginella* species, *S. haematodes* (Kunze) Spring and *S. pulcherrima* Liebm. using three independent methods: measurement of K_{shoot} by rehydration kinetics, and embolism resistance by X-ray computed tomography (micro-CT) and optical vulnerability (OV). These two species are native to rainforest understory and are morphologically representative of the majority of species in this genus, as well as most extinct species assigned to this genus over the past 400 million years (Rowe, 1988; Zhou *et al.*, 2016; Klaus *et al.*, 2017; Schmidt *et al.*, 2020). In addition to the hydraulic properties of the xylem, we also investigated stem anatomy and the efficiency and control of stomatal closure during drought. Furthermore, we compared measured xylem anatomical and hydraulic traits between these two species as a preliminary assessment of the variability in these key functional traits across closely related species in this genus.

Materials and Methods

Plant material

Potted individuals of *S. haematodes* and *S. pulcherrima* were grown in the glasshouse of the Botanical Garden of Ulm University. The conditions in the glasshouse were maintained at day/night temperatures above 18°C and under a natural, un-supplemented photoperiod. Plants received daily watering and a weekly application of liquid fertilizer. All experiments were conducted on the newest flush of fully expanded shoots during the summers of 2018 and 2019.

Stomatal responses to changes in water status

The relationship between stomatal conductance (g_s) and Ψ for each species was obtained from 30 branches harvested from three individuals per species that were excised and exposed to slow bench dehydration, under natural diffuse light, to ensure a controlled collection of data across the range of relevant Ψ . In addition, this relationship was supplemented from data collected from three intact potted plants in which water was withheld, to confirm that these relationships were similar in plants during natural drought (no significant difference in the relationships was observed). Measurements of Ψ and instantaneous g_s were

simultaneously carried out periodically by using a Scholander pressure chamber and infrared gas analyzer (LI-6400; Li-Cor, Lincoln, NE, USA). For g_s measurements, conditions in the leaf cuvette were controlled at a light intensity of $1000 \mu\text{mol m}^{-2} \text{s}^{-1}$, 25°C , $400 \mu\text{mol mol}^{-1} \text{CO}_2$ concentration and a leaf-to-air vapor pressure difference (VPD) of 1 kPa. Gas exchange measurements were normalized by surface area of leaves in the chamber, which were scanned after measurement.

Stomatal sensitivity to endogenous ABA during drought was also examined. Leaf gas exchange was measured in shoots from three unstressed plants during the morning (09:00–10:00 h) using the LI-6400 with the cuvette conditions set as previously described. After measuring leaf gas exchange, side shoots were sampled for Ψ and ABA quantification. Plants were then exposed to natural drought by withholding water for 18 d, during which time leaf gas exchange was measured periodically. After 18 d of withholding water, steady-state g_s had reached a minimum. In three shoots per species from three plants, leaf gas exchange was measured continuously and a side shoot was taken for the measurement of initial Ψ and ABA levels, the stem of the shoot was then excised under water and allowed to rehydrate. After *c.* 10 min the shoot had fully rehydrated and Ψ and ABA levels were again measured on a small side shoot. This experiment was designed to test whether stomatal closure during drought was driven by endogenous foliar ABA levels or leaf water status (McAdam & Brodribb, 2012; Cardoso & McAdam, 2019).

For ABA quantification, the excised side shoots were weighed ($\pm 0.0001 \text{ g}$) and covered in cold (-20°C) 80% (v/v) methanol in water and stored immediately at -20°C . Samples were freighted to Purdue University in the dark at room temperature, and ABA was extracted, purified and quantified by physicochemical methods using an added internal standard with an Agilent 6400 Series Triple Quadrupole liquid chromatograph associated with a tandem mass spectrometer according to the methods of McAdam (2015). ABA levels were expressed in terms of dry weight, which was quantified after ABA determination by weighing the dry mass of the sample harvested and extracted for analysis.

Whole shoot hydraulic vulnerability curves

Hydraulic vulnerability curves for each species were constructed by dehydrating plants on a bench and assessing K_{shoot} by the two-point rehydration method (Brodribb & Holbrook, 2003). Briefly, three well-watered potted plants from each species were taken into the laboratory early in the morning, and shoots with attached rhizome were removed from soil and desiccated slowly. The shoots were next bagged and placed in the dark for at least 15 min to reduce transpiration and promote equilibration in Ψ across the plant. Initial Ψ was assessed in a side branch using a Scholander pressure chamber (PMS Instrument Co., Albany, OR, USA), after which the shoot was excised under water and rehydrated for a period of time (10–240 s) enough to result in a final Ψ that was approximately half the initial value. For each sample, K_{shoot} was calculated from the following equation:

$$K_{\text{shoot}} = C_{\text{shoot}} \ln[\Psi_{\text{initial}}/\Psi_{\text{final}}]/t$$

Mean shoot capacitance (C_{shoot}) used for this calculation was determined both before and after turgor loss point for each species by pressure–volume curves, which were performed as described by Tyree & Hammel (1972). Briefly, six fully hydrated shoots, two taken from each of three individuals, were allowed to dehydrate as mass and Ψ were periodically measured. We calculated C_{shoot} from the linear slope of the relationship between relative water content and Ψ^{-1} before and following turgor loss point, and normalized by leaf area. K_{shoot} was determined using the C_{shoot} value calculated either before or following turgor loss point depending on the initial Ψ .

Optical vulnerability to embolism

Vulnerability curves for each species were assessed by the optical method (Brodribb *et al.*, 2016a). Three shoots, each taken from a separate individual, were excised from well-watered potted plants, and a paradermal section was made of the stem, with care taken to avoid all contact with the central vascular trace. Shoot excision did not induce embolism as both species had xylem consisting of short tracheids, and paradermal sections were made at least 15 cm from the cut end, to avoid artifacts. Once the paradermal section had exposed the central vascular trace the shoot was taped firmly to a glass slide and the exposed xylem was covered in jelly (Tensive conductive adhesive gel) on which a cover slip was placed. The area of exposed xylem was imaged under a stereomicroscope or compound microscope, with images taken every 180 s as the shoot dehydrated. Ψ was measured from excised small side branches (at least six per shoot) periodically during dehydration in a Scholander chamber until complete stem xylem embolism was obtained, Ψ was plotted against time and a linear regression was fitted to build a relationship that could be used to extrapolate Ψ for each embolism event, similar to Brodribb *et al.* (2016). Embolism was determined by a visible change in color in xylem conduits. The area of embolism was quantified by image subtraction of stacks of images using IMAGEJ, movements of stems and bubbles in the jelly were removed from the analysis. Complete descriptive details of this method are available on the open source website <http://www.opensourceov.org>. We plotted cumulative embolism area (as a percentage of total embolized area) against Ψ , with no curve fitting. Embolism was quantified as a percentage of the total embolized pixel area at the end of the dry-down period, and $P_{50\text{-optical}}$ (Ψ at which 50% embolized xylem area occurred using the optical method) was calculated as the statistical mean from the three curves.

Micro-CT vulnerability and imaging of internal stem anatomy during dehydration

Direct visualization of xylem embolism in intact plants over the course of dehydration was performed at the PSICHÉ beamline of the SOLEIL synchrotron (King *et al.*, 2016). Dehydration was induced by submitting potted plants to water withholding for *c.* 1–2 d. Shoots of each plant ($n = 20$ taken from across three plants

per species) were scanned more than 10 cm above emergence from the soil, using a high-flux ($3.1011 \text{ photons mm}^{-1}$) 25-keV monochromatic X-ray beam, while being rotated from 0° to 180° using a continuous rotation mode. The X-ray projections were collected with a 50-ms exposure time during rotation and recorded with an Orca-flash sCMOS camera (Hamamatsu Photonics KK, Shizuoka, Japan) equipped with a 250- μm -thick LuAG scintillator. Scan time was 75 s for each sample and yielded a stack of 1500 TIFF image slices. Fields of view were 3.13 mm^2 at a resolution of 2048×2048 pixels per slice. Vulnerability curves were constructed from shoots scanned only once. Tomographic reconstructions were conducted using the Paganin method (Paganin *et al.*, 2002) in PyHST2 software (Mirone *et al.*, 2014) and resulted in 2-bit volumic images with a $3.02\text{-}\mu\text{m}^3$ voxel resolution.

Before each scan, Ψ was measured with a Scholander pressure chamber (Model 1000, PMS Instrument Co.; DGMeca, Gradignan, France) from a small side branch. Quantification of embolized xylem area was conducted for each scan from a transverse cross-section taken from the center of the scan volume, and the percentage of embolized xylem area was quantified from the total tracheid area of the scan.

To test for the capacity of the cortex to rehydrate, a shoot sample with a small percentage of embolized tracheids was bagged and the cut end was excised under water following scanning. The shoot was rehydrated through the stem overnight. The following morning, Ψ was measured on a small side branch and the shoot was rescanned 10 mm below the point of the initial scan to avoid any areas of damage caused by the earlier scan (Petruzzellis *et al.*, 2018).

Micro-CT images were used to calculate the mean cortical volume lost in dehydrated stems before the mean onset of embolism, which was determined from optical vulnerability curves. This volume was calculated from the cross-sectional shoot area that was shrunken multiplied by the length of each shoot. This volume was expressed in terms of volume per unit area of shoot, and shoot area was measured by scanning shoots. The effect of VPD on the time taken until first embolism formation in the xylem was calculated using mean cortical area and the following equation:

$$\begin{aligned} &\text{Time to first embolism} \\ &= \frac{\text{Cortical volume lost}}{\left(\frac{\text{VPD}}{P_a} \times \text{minimum stomatal conductance}\right)} \end{aligned}$$

where P_a is atmospheric pressure and minimum stomatal conductance was taken from measurements of drought-stressed and bench-dried branches.

Shoot anatomy

The thickness of pit membranes between adjacent tracheids in the xylem of *S. haematodes* and *S. pulcherrima* was measured based on transmission electron microscopy (TEM) following a standard protocol (Zhang *et al.*, 2020). Samples from a single

plant per species were prepared. Briefly, small xylem blocks ($1 \times 2 \times 2 \text{ mm}$) were cut in water, fixed in 2.5% glutaraldehyde-buffered solution, post-fixed in 2% aqueous osmium tetroxide solution, stained *en bloc* in uranyl acetate, dehydrated in an ethanol series and embedded in Epon resin (Sigma Aldrich). Transverse semithin (500 nm) and ultrathin sections (60–100 nm) were cut using an ultramicrotome (Leica Ultracut UCT, Leica Microsystems) and placed on copper grids (Athena; Plano GmbH, Wetzlar, Germany). TEM images were taken with a JEM-1210 microscope at 120 kV (Jeol, Tokyo, Japan). Pit membrane thickness represented the mean of 50 individual pit membranes measured. The mean of three thickness measurements from the center to the annulus was taken for each individual pit membrane.

The tangential diameter of tracheids were measured as in Scholz *et al.* (2013) based on transverse sections of three individuals per species. Sections were prepared with a microtome (G.S.L.1 microtome; Schenkung Dapples, Zürich, Switzerland), or sectioned by hand with a razor blade, stained with safranin and astra blue, and observed with a light microscope (Zeiss AXIO Scope.A1, Zeiss). Images were taken with an Axiocam 305 color camera (Zeiss).

Light and fluorescence microscopy were used to examine the cell wall composition of the various tissues and cell types in the shoot of both species. Transverse sections of 30 μm were cut from the center of the shoot using the same microtome as mentioned above for three individual plants per species. Sections from the three individuals per species were randomly mixed in Petri dishes until further staining and observation was applied. At least five randomly selected sections per species were analysed to validate the staining patterns. Sections were stained for 15 min in 0.01% (w/v) aqueous Ruthenium Red (Merck KGaA, Billerica, MA, USA) solution to stain unesterified pectins (Sterling, 1970) and imaged with a light microscope (Axio Lab.A1, Axiocam ERc 5s; Zeiss) in bright field mode. Subsequently, the same sections were transferred for 5 min to an aqueous 0.5% (w/v) Astra Blue (Sigma-Aldrich, Munich, Germany) in 2% (w/v) aqueous tartaric acid (Merck Schuchardt OHG, Hohenbrunn, Germany) solution to stain hemicelluloses, except for mannans. Other sections were either stained for 15 min with a 0.03% (w/v) aqueous Coriphosphine O (Sigma Aldrich) solution to stain esterified pectins (de Oliveira *et al.*, 2014; Weis *et al.*, 1988), or for 5 min with saturated Auramine O (Schmid GmbH & Co, Freudensstadt, Germany) solution to stain lignified cell walls, cutin and suberin (Considine & Knox, 1979; Biggs & Miles, 1984, 1988; Ursache *et al.*, 2018). False color images of the Auramine O-stained sections were taken at 460–500 nm excitation and 512–542 nm emission (dichromatic mirror DC 505 nm) using a fluorescence microscope (CTR600, DMC 2900, DFC 3000 G; Leica, Wetzlar, Germany). To be able to discriminate the different wavelength bands emitted from Coriphosphine O sections, true color images were taken at an excitation of 390–410 nm and 487–503 nm, and an emission of 455–475, 515–545 and 620–660 nm (DC 415, 510, 590 nm). Unstained sections of both species were used as background to adjust exposure and to ensure that no signal was due to autofluorescence. The signals from weak

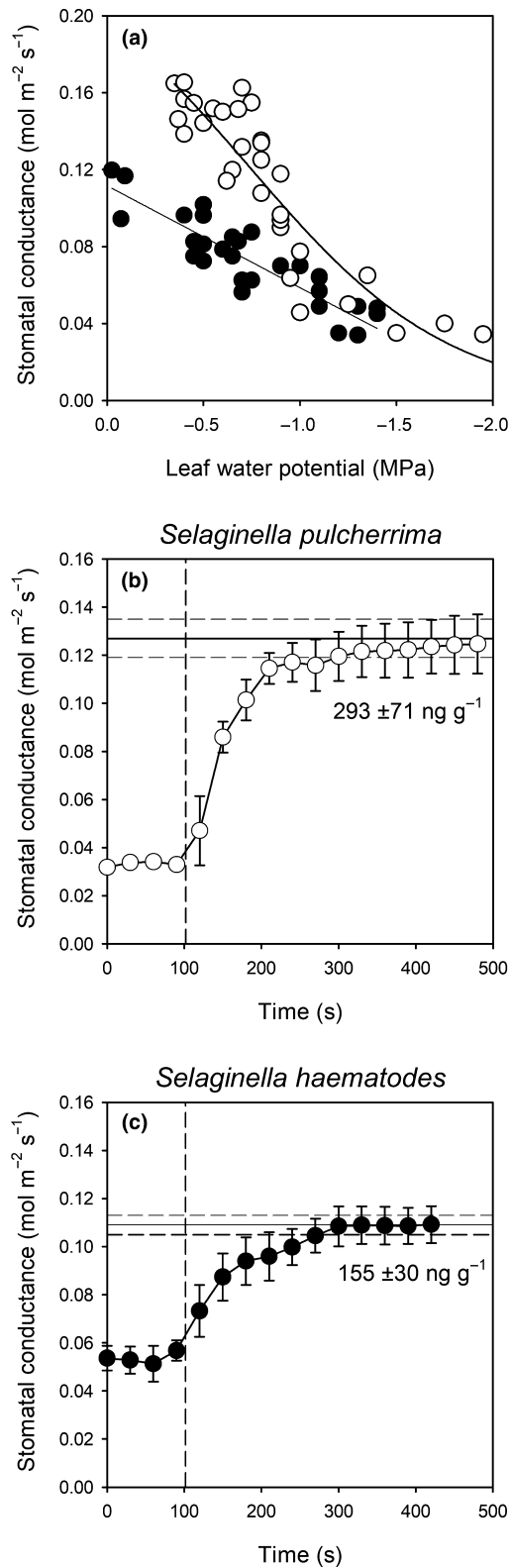


Fig. 1 (a) The relationship between stomatal conductance and shoot water potential for *Selaginella haematodes* (closed circles) and *S. pulcherrima* (open circles). Lines depict respective linear or sigmoidal regressions. The response of mean stomatal conductance ($n = 3$, \pm SE) to instantaneous rehydration (marked by the vertical dashed lines) in drought-stressed individuals of *S. pulcherrima* (b) and *S. haematodes* (c) (mean water potential before rehydration was -2.05 and -1.27 MPa for *S. pulcherrima* and *S. haematodes*, respectively). Mean stomatal conductance before drought in the same branches (solid horizontal gray line) \pm SE (dotted gray lines) are depicted. Mean endogenous foliar ABA levels (expressed in terms of DW) measured after gas exchange stability are shown. Equations for regressions are given in Supporting Information Table S1.

dye residues were visible in the washing solution. The stained sections were mounted in water on microscope slides, and coverslips were sealed with transparent nail polish (except for staining with Ruthenium Red). Images were analysed and edited with IMAGEJ.

Data analysis

$P_{50\text{-optical}}$ was taken directly from each of the optical vulnerability curves, as the Ψ at which 50% of the xylem area was embolized, and the mean for each species was then calculated from the values from the three shoots measured. The Ψ at which 50% of the xylem was embolized observed using micro-CT ($P_{50\text{-}\mu\text{CT}}$) and standard errors were determined using a sigmoidal function fitted using SIGMAPLOT software v.10 (Systat Software, Chicago, IL, USA). Generalized additive models and 95% confidence intervals were fitted to cortical separation data using the GAM function in the MGCV package of R software (R Core Team, 2019). Student's t -tests were used to test for differences in xylem anatomical and hydraulic traits between species.

Results

Despite differences in both the maximum rates of leaf gas exchange between the two *Selaginella* species and the sensitivity of stomata to Ψ , minimum measured g_s occurred in both species once Ψ had declined to -1.5 MPa in drought-stressed intact plants and bench-dried branches (Fig. 1a). Minimum g_s in both intact plants and bench-dried branches was 0.033 mol m⁻² s⁻¹ in *S. haematodes* and 0.035 mol m⁻² s⁻¹ in *S. pulcherrima*. These were $c.$ 28% of maximum rates of gas exchange in *S. haematodes* and 21% in *S. pulcherrima*. In both species, endogenous ABA synthesized during drought stress played no role in closing stomata during drought, as we found that stomata reopened to maximum measured apertures rapidly after instantaneous rehydration, despite high endogenous ABA levels in the leaf. Mean foliar ABA levels during drought were 155 and 293 ng g⁻¹ DW in *S. haematodes* and *S. pulcherrima*, respectively (compared to means of 130 and 119 ng g⁻¹ DW, respectively in unstressed leaves) (Fig. 1b,c).

The shoot hydraulic properties of the two species of *Selaginella* differed considerably. A three-fold difference in maximum K_{shoot} was observed between the two species, with a maximum K_{shoot} of 13.06 mmol m⁻² s⁻¹ MPa⁻¹ in *S. haematodes* and 28.93 mmol m⁻² s⁻¹ MPa⁻¹ in *S. pulcherrima* (Fig. 2a,c;

lignin and cellulose autofluorescence were captured by long exposure times at an excitation of 340–380 nm and an emission of 450–490 nm (DC 400 nm). All images were taken on the day that the staining was performed. Dyes were washed off the sections with water at least three times for about 1 min, or until no

Table 1). In both species, there was a range of Ψ over which K_{shoot} did not decline, but in both species increasingly negative Ψ led to a sigmoidal decline in K_{shoot} . Variation in hydraulic vulnerability, or the sensitivity of K_{shoot} to Ψ , was observed between the two species, with a 50% decline in K_{shoot} ($P_{50\text{-hydraulic}}$) occurring at -1.43 MPa for *S. haematodes* and -2.23 MPa for *S. pulcherrima* (Fig. 2a,c; Table 1).

The Ψ at which embolism formed in the xylem was considerably more negative than $P_{50\text{-hydraulic}}$. The first embolism events were only observed, both optically and by micro-CT, once Ψ had declined to a point at which K_{shoot} had decreased by more than 80% of maximum (Fig. 2a,c; Table 1). In *S. haematodes*, the mean Ψ at which the first embolism was optically observed was -2.48 MPa and in *S. pulcherrima* at -2.87 MPa (Fig. 2a,c; Table 1). As Ψ declined, more xylem area became embolized, with $P_{50\text{-optical}}$ being -2.98 MPa in *S. haematodes* and -4.57 MPa in *S. pulcherrima* (Fig. 2a,c; Table 1), while $P_{50\text{-}\mu\text{CT}}$ was -3.57 and -4.69 MPa, respectively. A broadly similar area of embolized xylem, as Ψ declined, was observed using the optical method and micro-CT scans (Fig. 2a,c).

Micro-CT imaging of intact stems revealed that decreasing Ψ caused a separation of the cortex from both the vascular cylinder and the leaf traces, and major shrinking of inner cortical cells in both species (Figs 2, 3). The resulting air-filled lacuna in both species was observed at reasonably high Ψ (-1.55 MPa for *S. haematodes* and -2 MPa for *S. pulcherrima*), and did not correspond to the Ψ at which embolism was first observed in the xylem optically or by micro-CT (Fig. 2b,d). By contrast, the Ψ at which the separation of the cortex from the vascular cylinder occurred corresponded to the Ψ that marked the onset of a decline in K_{shoot} (Fig. 4). As Ψ and K_{shoot} declined, the air-filled lacuna expanded to more than 20% of the cross-sectional area of the stem before the formation of embolism in the xylem (Fig. 4). Despite the large size of the air-filled lacuna isolating the cortex from the xylem, cellular connections between these two tissues were maintained by dispersed trabeculae (Fig. 3b). Once Ψ had declined sufficiently to trigger the formation of embolism in the xylem, more than 20% of the cross-sectional area of the stem was air-filled lacuna (Fig. 3a,b). Using the micro-CT images, we further calculated for both species the volume of water per unit leaf area that was expected to be available from cortex shrinkage, especially given that we saw no change in the outer diameter of stems. This was calculated from the area shrunken and the average length of the shoot, from the initiation of drought to the onset of embolism. This cortical shrinkage in *S. haematodes* stems was found to be sufficient to supply 8.825 mol of water per m^{-2} of leaf area, while in *S. pulcherrima* it would supply 16.586 mol of water per m^{-2} of leaf area before the formation of embolism. Over the same period relative water content in shoots declined to less than 50% before the onset of leaf embolism (Fig. 3c,d). Rehydration overnight was able to reverse the formation of the air-filled lacuna before the formation of embolism in the xylem (Fig. S2).

Xylem anatomy varied little between the two *Selaginella* species, with only tracheid diameter being significantly narrower in *S. pulcherrima* compared to *S. haematodes* (Table 1).

Microscopy revealed differences in cell wall thickness and chemical composition between the epidermis, outer and inner cortex, pericycle, phloem and xylem tissues (Fig. 5). In both species, the lignin signals were largely similar based on Auramine O and autofluorescence at 340–380 nm excitation (Fig. 5a), but different intensities were visualized across tissues. Both species showed strongest lignin signals in xylem, and strong Auramine O signals were also found in the cortex, especially in the thick-walled outer cortex and hypodermis. In addition, the cuticular and/or outer epidermis, and the pericycle exhibited strong autofluorescence signals at 340–380 nm excitation (Fig. 5a), which was most pronounced in *S. pulcherrima*, and also visible at leaf traces (arrows in Fig. 5a). The differences between the two lignin visualization techniques suggest that the xylem and nonxylem tissue have different lignin compositions, which is in line with Weng *et al.*, (2008), who reported *p*-hydroxyphenyl (H), guaiacyl (G) lignin and syringyl (S) lignin in the cortex, but mainly G lignin with traces of S lignin for the xylem of *Selaginella moellendorffii*. The green emitted light after Coriphosphine O treatment was largely found at the same locations (i.e. xylem and outer cortex) and with comparable relative intensities as the Auramine O signals (Fig. 5a,b).

Astra Blue, which is characteristic for hemicellulose except for mannans, stained all tissues but not the xylem (Fig. 5c–e). The strongest hemicellulose signals were found in the phloem and pericycle of both *Selaginella* species (Fig. 5d), but *S. pulcherrima* also displayed Astra Blue signals in the inner cortex close to the stele (Fig. 5e). Red Coriphosphine O signals and Ruthenium Red signals, which stain esterified and unesterified pectins, respectively, were present in the inner cortex (Fig. 5b) and endodermis (Fig. 5f). Ruthenium Red stained the phloem, pericycle, endodermal trabeculae (Fig. 5f), inner and outer cortex, and the epidermis. Only a weak Coriphosphine O pectin signal was visible in the xylem as well as in the outer cortex and epidermis (yellow, mixed colours in Fig. 5b), suggesting different distribution of the two pectin types. The trabeculae were the only structures not having any lignin signals in contrast to the xylem tracheids, which showed no hemicellulose (Fig. 5c–e), the lowest pectin signals (Fig. 5c,f) and the strongest lignin signals (Fig. 5a,b).

Discussion

The risk of hydraulic failure during acute water stress is known to place limits on the geographic distribution of species (Choat *et al.*, 2012), such that in seed plants embolism resistance can be linked to water availability and life history strategy. The native habitat of the majority of terrestrial *Selaginella* species, and previously described xylem anatomical and functional traits in these species, suggest that *Selaginella* species are not highly resistant to embolism formation. Here, we demonstrate that the xylem conduits in two terrestrial *Selaginella* species, native to tropical rainforest, are more resistant than expected based on plant habitat or hydraulic vulnerability curves (Brodribb & Holbrook, 2004). We encountered a sequence of events occurring in *Selaginella* as drought progressed: stomatal closure, separation of the cortex from the vascular cylinder

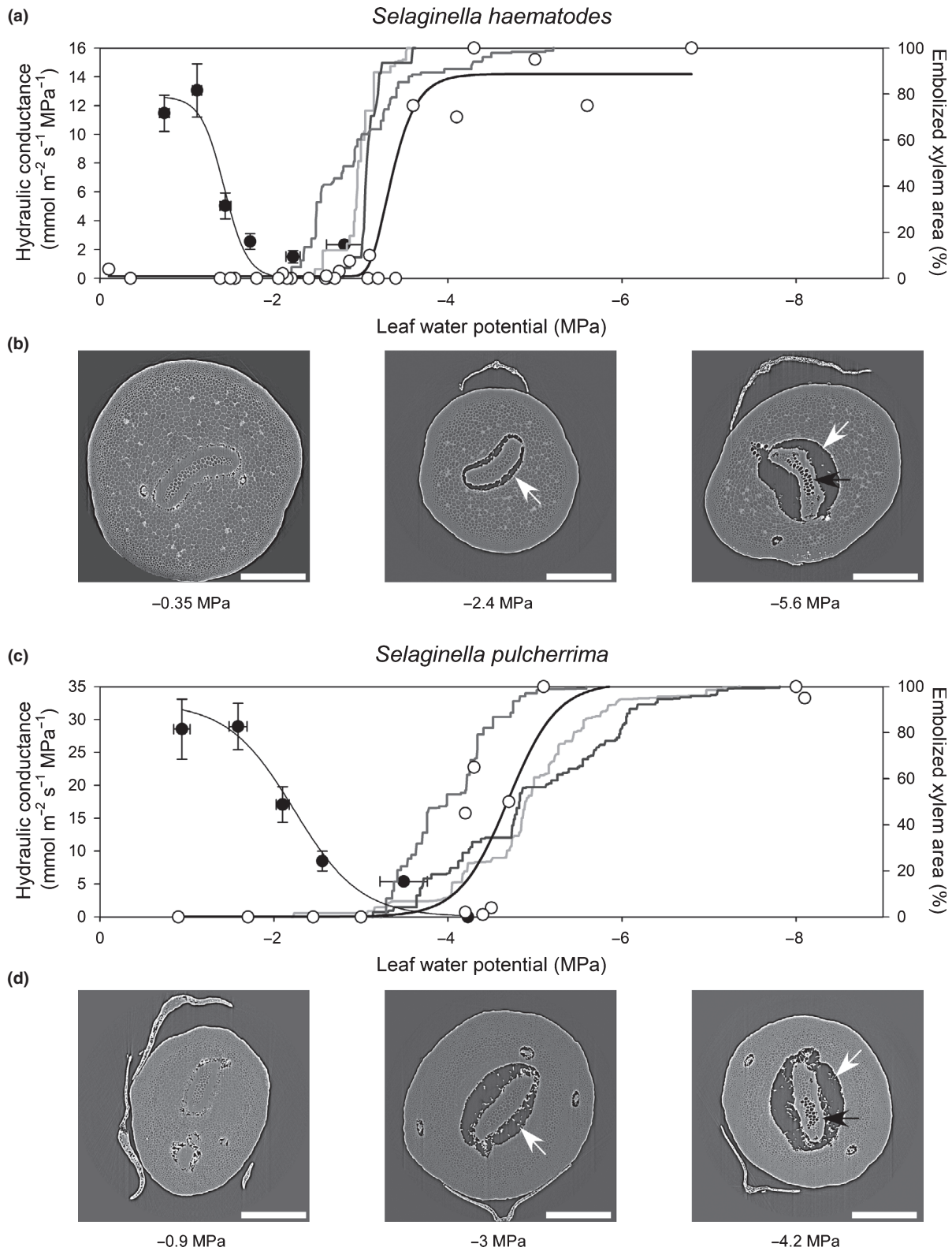


Fig. 2 The response of mean shoot hydraulic conductance (closed circles, \pm SE, regressions in fine black lines), accumulated percentage of embolized xylem area observed in three stems based on the optical method (gray lines) and embolized cross-sectional xylem area observed by micro-CT (open circles, regressions in heavy black) to a decline in leaf water potential in *Selaginella haematodes* (a) and *S. pulcherrima* (c). Representative transverse images of shoots during desiccation are depicted for *S. haematodes* (b) and *S. pulcherrima* (d); labels below correspond to the water potential at which the shoot was scanned, white arrows indicate the air-filled lacuna and black arrows indicate embolized tracheids (bar, 500 μ m). Equations for regressions are given in Supporting Information Table S1.

Table 1 Mean ($n = 50$, \pm SE) xylem anatomical and hydraulic traits measured in the shoots of *Selaginella haematodes* and *S. pulcherrima*; P -values for Student's t -tests are also shown.

Trait	<i>S. haematodes</i>		<i>S. pulcherrima</i>		P -value
	Mean	SE	Mean	SE	
Pit membrane thickness (nm)	262	75	310	60	0.61
Tracheid diameter (μm)	20.61	2.05	17.44	0.99	0.17
Hydraulic tracheid diameter (μm)	11.97	0.78	9.7	0.79	0.04
Maximum K_{shoot} ($\text{mmol m}^{-2} \text{s}^{-1} \text{MPa}^{-1}$)	13.06	1.85	28.93	3.54	<0.0001
Ψ of first optical embolism	-2.48	0.16	-2.87	0.32	0.33
$P_{50\text{-hydraulic}}$ (MPa)	-1.43	0.27	-2.23	0.34	<0.01
$P_{50\text{-optical}}$ (MPa)	-2.98	0.04	-4.57	0.29	0.006
$P_{50\text{-}\mu\text{CT}}$ (MPa)	-3.57	0.12	-4.69	0.25	<0.001

concomitant with declines in whole K_{shoot} , a reduction in cortical cell volume, and finally the formation of embolism in the stem xylem.

Declines in hydraulic conductance and embolism formation

Maximum rates of K_{shoot} and g_s in the two *Selaginella* species measured here are similar to those reported in some angiosperms (Brodrribb & Holbrook, 2004; Sack & Holbrook, 2006). The difference in K_{shoot} between both species corresponded to species differences in maximum rates of leaf gas exchange, with *S. pulcherrima* having the highest K_{shoot} and g_s . In most seed plant species, declines in K_{shoot} are associated with the formation of embolism in the xylem (Brodrribb *et al.*, 2016b), but declines in hydraulic conductance driven by changes to the pathways of water outside the xylem have also been reported to occur at high Ψ in angiosperm leaves (Scoffoni *et al.*, 2017) and roots (Cuneo *et al.*, 2016, 2020). Here we demonstrate that considerable (up to 80%) reductions in K_{shoot} in two *Selaginella* species precede embolism formation. Visualization of the internal anatomy of the stem by micro-CT revealed that, similar to desiccation-tolerant ferns (Holmlund *et al.*, 2019), a physical separation between the cortex and the vascular cylinder occurred when Ψ declines in *Selaginella*. Unlike in desiccation-tolerant ferns, the large, air-

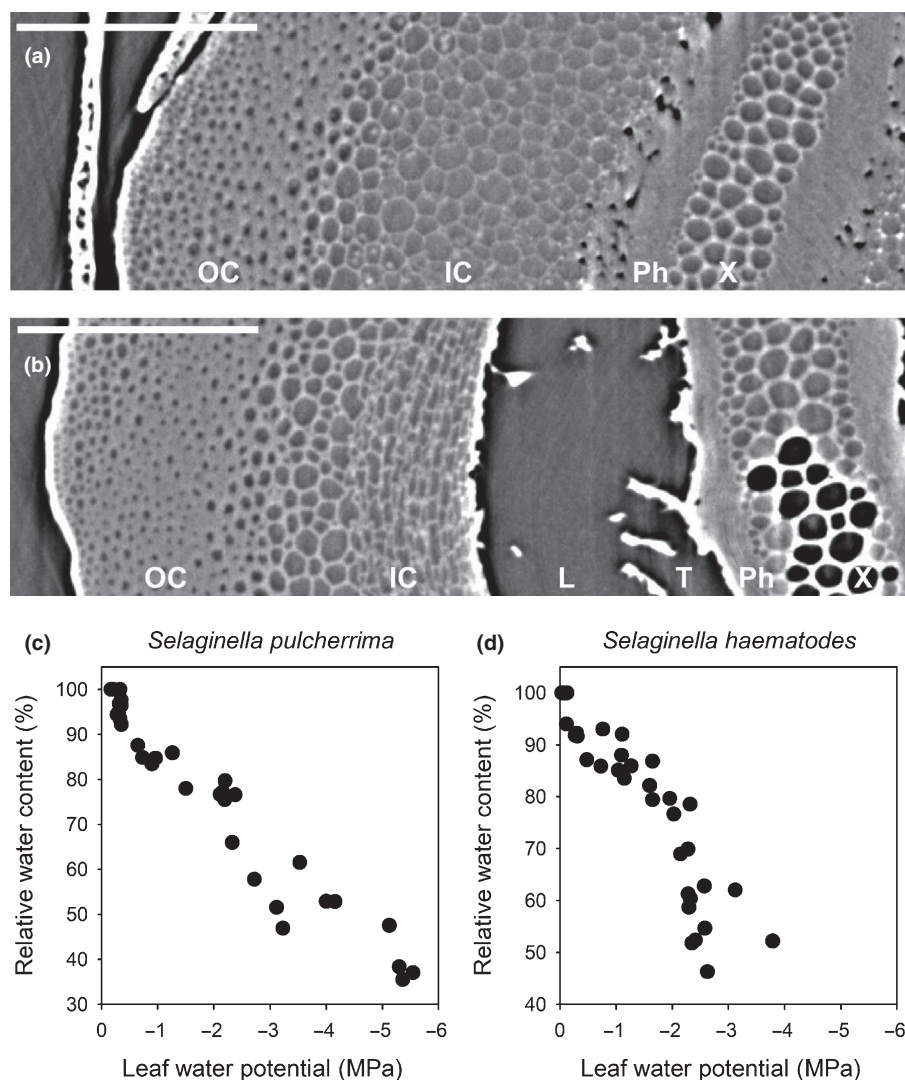


Fig. 3 Transverse slices from micro-CT scans of a stem of *Selaginella pulcherrima* at a moderate water potential (-0.8 MPa) (a) and the same stem dehydrated to -4.1 MPa (b) scanned 10 mm below the original scanned area. Considerable shrinkage of cortical cells and separation of the cortex from the central vascular cylinder can be seen in the dehydrated stem as well as embolized xylem elements and trabeculae traversing the lacuna (scale bar = $200 \mu\text{m}$). OC, outer cortex; IC, inner cortex; L, lacuna; T, trabeculae; Ph, phloem; X, xylem. Pressure-volume curves for *S. pulcherrima* (c) and *S. haematodes* (d) (data pooled from five shoots).

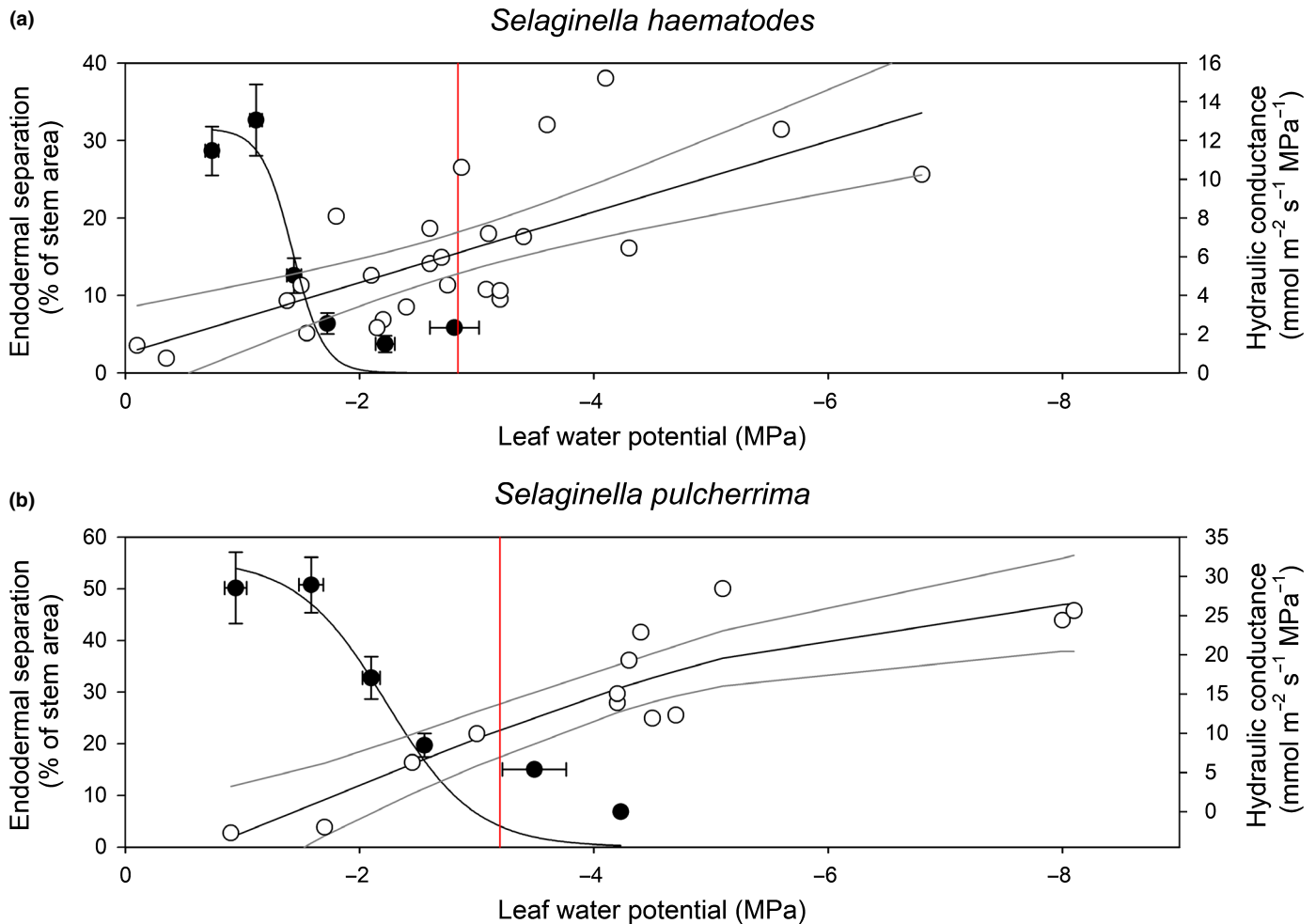


Fig. 4 The degree of endodermal separation or lacuna cross-sectional area, as a percentage of stem cross-sectional area (open circles), and the response of mean shoot hydraulic conductance (closed circles, \pm SE) to declines in leaf water potential for *Selaginella haematodes* (a) and *S. pulcherrima* (b). Black lines depict generalized additive models with gray lines depicting the bands of the 95% confidence interval. The vertical red line represents the mean water potential of incipient embolism in the xylem observed by the optical method.

filled lacuna in *Selaginella* forms at high Ψ before embolism formation and is the result of water loss and cell collapse in the cortex, not from the vascular tissue collapsing within the vascular cylinder. We suggest that the formation of this air-filled lacuna during dehydration is the primary cause for the 80% reduction in K_{shoot} before the onset of embolism in these two species of *Selaginella*. This is similar to the separation and collapse of the cortex in *Vitis* roots leading to substantial declines in root hydraulic conductance in the early stages of drought (Cuneo *et al.*, 2016, 2020). We also suggest that the limited connection through trabeculae between the vasculature and the cortical tissues probably accounts for the observed lack of complete decline in K_{shoot} until embolism formation. In *Selaginella*, for xylem water to irrigate photosynthetic tissue it must traverse the endodermis via these trabeculae. Declines in outside-xylem hydraulic conductance due to reduced membrane permeability, which was not assessed in this study, cannot be ruled out as an additive explanation for declines in K_{shoot} (Scoffoni *et al.*, 2017). These events have only been observed in angiosperms at high Ψ , and in both

Selaginella species measured here we report a period of declining Ψ to -2 MPa where we observed no decline in K_{shoot} .

Given that both species in our study are native to tropical rainforest understory environments, where periods of soil water deficit are exceptionally rare, we hypothesize that the large volume of water lost from cortical collapse plays a critical role in extending the period of time these plants can survive excursions in VPD. We calculated the time taken for stems to lose this cortical water, and therefore reach a Ψ sufficient to induce embolism, in the absence of recharge from soil water. We found that *S. pulcherrima* is likely to survive a VPD of 3 kPa for 4.3 h, solely on the supply of water from the cortex, while *S. haematodes* could survive for 2.3 h (Fig. 6). These temporal ranges may seem limited, but are based on the unlikely assumptions that soil water potential was low, and the cortex of the extensive, underground rhizome did not contribute any water, and therefore they represent considerable underestimates of this time period. In addition to the unlikely event that these *Selaginella* species ever rely solely on cortical water for survival, excursions in VPD to this extreme, at ground level in the tropical understory are exceptionally rare,

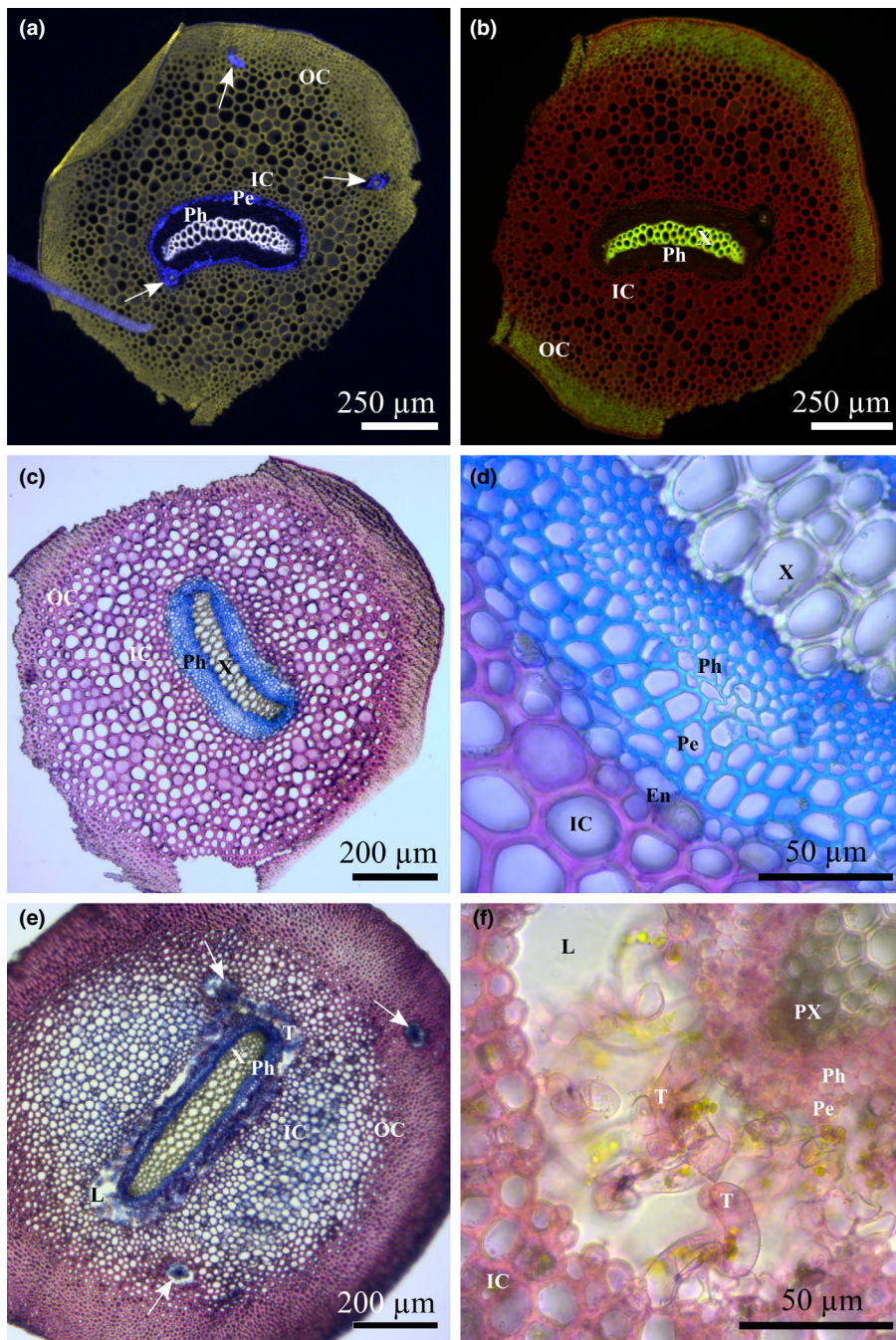


Fig. 5 Light and fluorescence images of stem cross-sections of *Selaginella haematodes* (a–d) and *S. pulcherrima* (e, f) after staining with Auramine O (lignin; a), Coriphosphine O (esterified pectins; b), Ruthenium Red (unesterified pectins; c–f), Astra blue (hemicellulose; c–e), lignin autofluorescence was captured at 450–490 nm under UV excitation (a). A false color image is shown in (a) (yellow = auramine; blue = autofluorescence; bright white = merged strong signals), while (b) represents a true color image (orange and red = pectin, bright green = lignified cell walls of xylem). Arrows in (a) and (e) point to leaf traces. Chloroplasts are visible as green, granular structures in (f). OC, outer cortex; IC, inner cortex; Pe, pericycle; Ph, phloem; X, xylem; En, endodermis; T, trabeculae; L, lacunar cavity; PX, protoxylem.

or nonexistent, with the highest VPD in such environments rarely exceeding 1.5 kPa (Motzer *et al.*, 2005; Bujan *et al.*, 2016). At a VPD of 1.5 kPa, these species could survive on cortical water alone for 10 and 5 h, respectively (Fig. 6). Consequently, we would argue that cortical collapse and resistant xylem together provides the ideal mechanism for *Selaginella* plants to survive diurnal excursions in VPD, or even short periods of soil water deficit, with stomata that cannot close sufficiently. It is also tempting to speculate that the highly resistant xylem of *Selaginella* may have also evolved to protect species from rare episodes of drought, which can also occur in tropical forests (Powers *et al.*, 2020).

The presence of pectins and hemicellulose in cortical cell walls may explain why the inner cortical cells of *Selaginella* are capable of losing a vast volume of water, and recovering on rehydration, as hemicellulose and pectins are known as cell wall compounds strongly responding to (de)hydration (Caffall & Mohnen, 2009; Voragen *et al.*, 2009; van Doorn *et al.*, 2011; Brulé *et al.*, 2019). Leroux *et al.* (2015) found hemicelluloses such as galactan and xyloglucan in the phloem, and xyloglucan as well as galactan in the cortex of *Selaginella grandis* based on immunohistochemistry, confirming our findings based on less specific stains. The stem xylem of the two *Selaginella* species was found to be surprisingly resistant to embolism formation, contrary to our initial

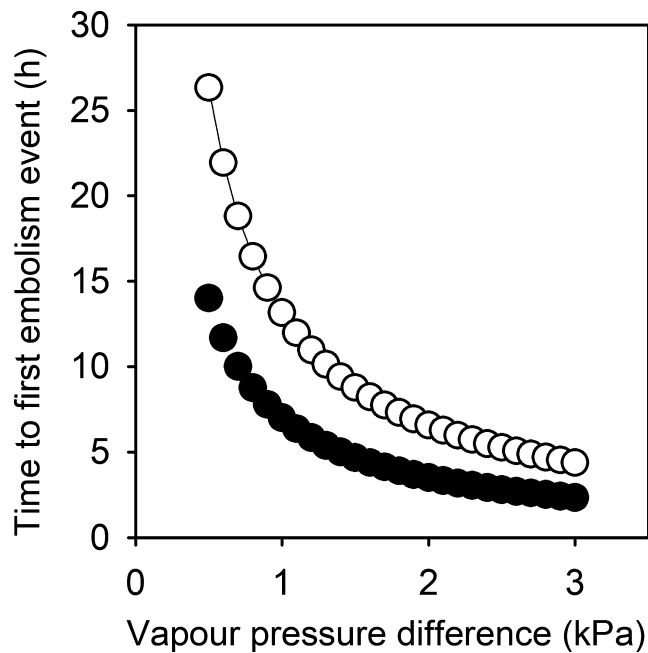


Fig. 6 The relationship between the time (h) taken for a stem to reach the water potential of incipient embolism and vapor pressure difference (kPa) in *Selaginella haematodes* (closed circles) and *S. pulcherrima* (open circles). The calculation of time assumes shoots rely solely on cortical water and not a supply from the soil, and that stomata were closed.

hypothesis based on published xylem traits, hydraulic function and habitat preferences of these two *Selaginella* species. Highly resistant xylem (xylem in which embolism does not form until at least -5 MPa) has been described for the stipes of several fern species (Pittermann *et al.*, 2011; Brodersen *et al.*, 2014, 2016), and here we further indicate two *Selaginella* species with xylem that does not embolize until -3.0 MPa. Such high xylem resistance to embolism formation in both *Selaginella* species may be due to relatively thick interconduit pit membranes. Both species fell on the relationship between embolism resistance and pit membrane thickness reported in angiosperms (Li *et al.*, 2016). Furthermore, syringyl (S) lignin is synthesized in species of *Selaginella*, following a different pathway from the biosynthetic pathway of seed plants (Weng *et al.*, 2008, 2010, 2011). The ratio of S:guaiacyl (G) monomers composing lignin has recently been related to embolism resistance and leaf lifespan in species native to seasonally dry rainforests, with species with high rates of S monomers forming lignin with high xylem resistance to embolism (Lima *et al.*, 2018). The differences we observed between the two lignin visualization techniques suggest that the xylem and nonxylem tissue in *Selaginella* have different lignin compositions, which is in line with Weng *et al.*, (2008), who reported *p*-hydroxyphenyl, G lignin and S lignin in the cortex, but mainly G lignin with traces of S lignin for the xylem of *Selaginella moellendorffii*.

A major question is why would species adapted to ever-wet tropical forests evolve xylem that is quite resistant to embolism (McElwain, 2011)? In angiosperms there can be a substantial variation in embolism resistance across species native to tropical rainforests (Trueba *et al.*, 2017; Zeiger *et al.*, 2019). In some

instances, this is because tropical rainforest species have distributions that extend into seasonally dry habitats (Trueba *et al.*, 2017). In *Selaginella* species it is likely that resistant xylem evolved because of inefficient stomatal closure, as a means of prolonging the period of time plants can draw upon cortical water after the imposition of high VPD and before the formation of lethal embolism. Given that resistant xylem has been observed in mesic species from the two earliest diverging extant vascular land plant clades (Pittermann *et al.*, 2011; Brodersen *et al.*, 2014, 2016), it is tempting to speculate that the earliest xylem in the common ancestor of vascular plants, and possibly the earliest plants on land, was equally resistant to embolism formation. We do not yet know what precise features of the xylem of *Selaginella* allow it to be so resistant to embolism formation. However, the lack of pre-existing air-filled tracheids in the xylem, from which embolism could spread during drought, might contribute to the high embolism resistance. In seed plants, the first embolism events are often observed near more vulnerable primary xylem (Choat *et al.*, 2016).

Early stomatal closure during leaf dehydration precedes declines in hydraulic conductance and xylem dysfunction

In both *Selaginella* species stomatal closure occurred before declines in both K_{shoot} and the formation of embolism. This mirrors observations across vascular land plants (Brodrribb & Holbrook, 2004; Martin-StPaul *et al.*, 2017; Creek *et al.*, 2020), and emphasizes the strong selective pressure for stomatal closure before embolism formation (Cardoso *et al.*, 2018). A striking difference between the observations of the two *Selaginella* species here and most other vascular plants is the high rate of minimum leaf conductance (>0.03 mol m⁻² s⁻¹). Given such high rates of minimum leaf conductance, which could either be due to incompletely closed stomata or a highly permeable cuticle (Duursma *et al.*, 2018), without a mobile pool of water like that found in the cortex, these two *Selaginella* species would probably be confined to an aquatic environment.

Like many species of lycophyte and fern (McAdam & Brodrribb, 2012; Cardoso *et al.*, 2019), the two species of *Selaginella* observed here have no appreciable stomatal sensitivity to endogenous ABA during drought, as demonstrated by the rapid increase in g_s response to instantaneous rehydration, despite high levels of ABA. The lack of stomatal sensitivity to endogenous ABA during drought is widely reported across the genus *Selaginella*, with similar observations documented in *Selaginella kraussiana* (McAdam & Brodrribb, 2012) and *Selaginella uncinata* (Brodrribb *et al.*, 2017), despite an early report of stomatal responses to exogenous ABA application in the latter species (Ruszala *et al.*, 2011). The ability of g_s in both *Selaginella* species to recover in minutes to maximum rates of gas exchange after instantaneous rehydration from a drought stressed state suggests that endodermal separation may repair rapidly on rehydration, although further work would be required to demonstrate this. It has been argued that the evolution of stomatal sensitivity to ABA was instrumental for lineages of seed plants to invade extremely dry, seasonal environments, without investing in highly resistant xylem. Species of *Pinus*, for instance, provide an excellent case supporting this

argument (Brodribb *et al.*, 2014). There are, however, many lycophyte and fern species that have extremely low rates of minimum leaf conductance, a trait commonly observed in epiphytic species, which tolerate periods of prolonged desiccation (Schuster *et al.*, 2017). There might be a stomatal safety–efficiency trade-off in species of early diverging vascular land plants that have a passive hydraulic regulation of stomatal aperture in response to changes in leaf water status, whereby species adopt either low maximum rates of gas exchange and concurrent low rates of minimum leaf conductance, or high rates of maximum gas exchange coupled with high rates of minimum leaf conductance (as observed here) (Henry *et al.*, 2019). Exploring exceptions to this stomatal efficiency–safety trade-off in species of early diverging vascular land plant is essential. The evolution of functional stomatal sensitivity to endogenous ABA in seed plants might have allowed them to escape this trade-off, attaining high rates of leaf gas exchange in seasonal environments, while relying on metabolic stomatal closure driven by ABA, to ensure minimum rates of leaf conductance during drought events.

Conclusion

Our results suggest that resistant xylem may be an ancestral trait in vascular plants and that large volumes of water lost from the cortex of the stem of *Selaginella* (up to 50% relative water content) probably sustains plants with high rates of minimum leaf conductance during excursions in VPD. A high capacitance in the cortex may also be an ancient strategy of vascular land plants. There is a well-documented and distinctive inner and outer cortex, reminiscent of the anatomy of *Selaginella* stems, found in the fossilized stems of the lycophyte ancestor *Asteroxylon* from the 400 million year old Rhynie Chert (Kidston & Lang, 1920). Further studies of embolism resistance across lycophytes and early diverging ferns will provide considerable insight into the origin and evolution of embolism resistance and drought survival mechanisms in vascular plants (Rowe, 1988; Klaus *et al.*, 2017).

Acknowledgements








The authors thank the PSICHÉ beamline (SOLEIL, France), and the Botanical Garden of Ulm University for providing and maintaining plant material, the US Department of Agriculture National Institute of Food and Agriculture (Hatch Project 1014908; SAMM), the Alexander von Humboldt Foundation for a postdoctoral fellowship to SAMM and four anonymous reviewers for helpful comments. Funding to LK and SJ was provided by the German Research Foundation (DFG project no. 383393940). We acknowledge the use of the Metabolite Profiling facility of the Bindley Bioscience Center, a core facility of the National Institute of Health–funded Indiana Clinical and Translational Sciences Institute, for assisting in the quantification of ABA levels.

Author contributions

SAMM with DV, AAC and SJ conceived the study; DV with CGS and SAMM collected optical vulnerability curves and xylem anatomical measurements; CNK and TAB collected pressure–volume curves; CNK with AAC performed gas exchange and ABA

measurements; LK conducted staining and anatomical imaging; YW, AK, JMT, HC, SD, AAC, DC, RB, EB and SAMM performed micro-CT experiments; SJ supervised anatomical aspects of the project; SAMM supervised all aspects of the project; AAC, LK and SAMM wrote the manuscript with help from all authors.

ORCID

Amanda A. Cardoso  <https://orcid.org/0000-0001-7078-6246>
 Hervé Cochard  <https://orcid.org/0000-0002-2727-7072>
 Déborah Corso  <https://orcid.org/0000-0002-3797-0153>
 Sylvain Delzon  <https://orcid.org/0000-0003-3442-1711>
 Steven Jansen  <https://orcid.org/0000-0002-4476-5334>
 Scott A. M. McAdam  <https://orcid.org/0000-0002-9625-6750>
 José M. Torres-Ruiz  <https://orcid.org/0000-0003-1367-7056>

References

- Ambrose BA. 2013. The morphology and development of lycophytes. *Annual Plant Reviews* 45: 91–114.
- Barclay BD. 1931. Origin and development of tissues in stem of *Selaginella wildenovii*. *Botanical Gazette* 91: 452–461.
- Biggs AR, Miles NW. 1984. Suberin deposition as a measure of wound response in peach bark. *HortScience* 20: 902–905.
- Biggs AR, Miles NW. 1988. Association of suberin formation in uninoculated wounds with susceptibility to *Leucostoma cincta* and *L. persoonii* in various peach cultivars. *Phytopathology* 78: 1070–1074.
- Brodersen C, Jansen S, Choat B, Rico C, Pittermann J. 2014. Cavitation resistance in seedless vascular plants: the structure and function of interconduit pit membranes. *Plant Physiology* 165: 895–904.
- Brodersen CR, Rico C, Guenni O, Pittermann J. 2016. Embolism spread in the primary xylem of *Polystichum munitum*: implications for water transport during seasonal drought. *Plant Cell & Environment* 39: 338–346.
- Brodribb TJ, Bienaimé D, Marmottant P. 2016a. Revealing catastrophic failure of leaf networks under stress. *Proceedings of the National Academy of Sciences, USA* 113: 4865–4869.
- Brodribb TJ, Cochard H. 2009. Hydraulic failure defines the recovery and point of death in water-stressed conifers. *Plant Physiology* 149: 575–584.
- Brodribb TJ, Holbrook NM. 2003. Stomatal closure during leaf dehydration, correlation with other leaf physiological traits. *Plant Physiology* 132: 2166–2173.
- Brodribb TJ, Holbrook NM. 2004. Stomatal protection against hydraulic failure: a comparison of coexisting ferns and angiosperms. *New Phytologist* 162: 663–670.
- Brodribb TJ, McAdam SAM. 2011. Passive origins of stomatal control. *Science* 331: 582–585.
- Brodribb TJ, McAdam SAM, Carins Murphy MR. 2017. Xylem and stomata are coordinated through time and space. *Plant, Cell & Environment*. 40: 872–880.
- Brodribb TJ, McAdam SAM, Jordan GJ, Martins SCV. 2014. Conifer species adapt to low-rainfall climates by following one of two divergent pathways. *Proceedings of the National Academy of Sciences, USA* 111: 14489–14493.
- Brodribb TJ, Skelton RP, McAdam SAM, Bienaimé D, Lucani CJ, Marmottant P. 2016b. Visual quantification of embolism reveals leaf vulnerability to hydraulic failure. *New Phytologist* 209: 1403–1409.
- Brulé V, Rafsanjani A, Asgari M, Western TL, Pasini D. 2019. Three-dimensional functional gradients direct stem curling in the resurrection plant *Selaginella lepidophylla*. *Journal of the Royal Society Interface* 16: 20190454.
- Buck WR, Lucansky TW. 1976. An anatomical and morphological comparison of *Selaginella apoda* and *Selaginella ludoviciana*. *Bulletin of the Torrey Botanical Club* 103: 9–16.
- Bujan J, Yanoviak SP, Kaspari M. 2016. Desiccation resistance in tropical insects: causes and mechanisms underlying variability in a Panama ant community. *Ecology and Evolution* 6: 6282–6291.

- Caffall KH, Mohnen D. 2009. The structure, function, and biosynthesis of plant cell wall pectic polysaccharides. *Carbohydrate Research* 344: 1879–1900.
- Campany CE, Martin L, Watkins JE. 2019. Convergence of ecophysiological traits drives floristic composition of early lineage vascular plants in a tropical forest floor. *Annals of Botany* 123: 793–803.
- Cardoso AA, Batz TA, McAdam SAM. 2020. Xylem embolism resistance determines leaf mortality during drought in *Persea americana*. *Plant Physiology* 182: 547–554.
- Cardoso AA, Brodribb TJ, Lucani CJ, DaMatta FM, McAdam SAM. 2018. Coordinated plasticity maintains hydraulic safety in sunflower leaves. *Plant, Cell & Environment* 41: 2567–2576.
- Cardoso AA, McAdam SAM. 2019. Misleading conclusions from exogenous ABA application: a cautionary tale about the evolution of stomatal responses to changes in leaf water status. *Plant Signaling and Behavior* 14: 1610307.
- Cardoso AA, Randall JM, McAdam SAM. 2019. Hydraulics regulate stomatal responses to changes in leaf water status in the fern *Athyrium filix-femina*. *Plant Physiology* 179: 533–543.
- Choat B, Badel E, Burtlett R, Delzon S, Cochard H, Jansen S. 2016. Noninvasive measurement of vulnerability to drought-induced embolism by x-ray microtomography. *Plant Physiology* 170: 273–282.
- Choat B, Jansen S, Brodribb TJ, Cochard H, Delzon S, Bhaskar R, Bucci SJ, Feild TS, Gleason SM, Hacke UG *et al.* 2012. Global convergence in the vulnerability of forests to drought. *Nature* 491: 752–755.
- Considine JA, Knox RB. 1979. Development and histochemistry of the cells, cell walls, and cuticle of the dermal system of fruit of the grape, *Vitis vinifera* L. *Protoplasma* 99: 347–365.
- Creek D, Lamarque LJ, Torres-Ruiz JM, Parise C, Burtlett R, Tissue DT, Delzon S. 2019. Xylem embolism in leaves does not occur with open stomata: evidence from direct observations using the optical visualization technique. *Journal of Experimental Botany* 71: 1151–1159.
- Cunéo IF, Barrios-Masias F, Knipfer T, Uretsky J, Reyes C, Lenain P, Brodersen CR, Walker MA, McElrone AJ. 2020. Differences in grapevine rootstock sensitivity and recovery from drought are linked to fine root cortical lacunae and root tip function. *New Phytologist*. doi: 10.1111/nph.16542.
- Cunéo IF, Knipfer T, Brodersen CR, McElrone AJ. 2016. Mechanical failure of fine root cortical cells initiates plant hydraulic decline during drought. *Plant Physiology* 172: 1669–1678.
- de Oliveira DC, Magalhães TA, Ferreira BG, Teixeira CT, Formiga AT, Fernandes GW, Isaias RMDs. 2014. Variation in the degree of pectin methylesterification during the development of *Baccharis dracunculifolia* kidney-shaped gall. *PLoS ONE* 9: e94588.
- Deans RM, Brodribb TJ, McAdam SAM. 2017. An integrated hydraulic–hormonal model of conifer stomata predicts water stress dynamics. *Plant Physiology* 174: 478–486.
- Duerden H. 1934. On the occurrence of vessels in *Selaginella*. *Annals of Botany* 48: 459–465.
- Duursma RA, Blackman CJ, López R, Martin-StPaul NK, Cochard H, Medlyn BE. 2018. On the minimum leaf conductance: its role in models of plant water use, and ecological and environmental controls. *New Phytologist* 221: 693–705.
- Franks PJ, Farquhar GD. 2007. The mechanical diversity of stomata and its significance in gas-exchange control. *Plant Physiology* 143: 78–87.
- Gola EM, Jernstedt JA. 2016. Vascular structure contributes to shoot sectoriality in *Selaginella kraussiana*. *Acta Societatis Botanicorum Poloniae* 85: 1–12.
- Henry C, John GP, Pan R, Bartlett MK, Fletcher LR, Scoffoni C, Sack L. 2019. A stomatal safety–efficiency trade-off constrains responses to leaf dehydration. *Nature Communications* 10: 3398.
- Holmlund HI, Pratt RB, Jacobsen AL, Davis SD, Pittermann J. 2019. High-resolution computed tomography reveals dynamics of desiccation and rehydration in fern petioles of a desiccation-tolerant fern. *New Phytologist* 224: 97–105.
- Kaack L, Altaner C, Carmesin C, Diaz A, Holler M, Kranz C, Neusser G, Odrštil M, Schenk HJ, Schmidt V *et al.* 2019. Function and three-dimensional structure of intervessel pit membranes in angiosperms: a review. *IAWA Journal* 40: 673–702.
- Kidston R, Lang WH. 1920. On Old Red Sandstone plants showing structure, from the Rhynie Chert Bed, Aberdeenshire: Part III. *Asteroxylon mackiei*, Kidston and Lang. *Royal Society of Edinburgh Transactions* 52: 643–680.
- King A, Guignot N, Zerbino P, Boulard E, Desjardins K, Bordessoule M, Leclerq N, Le S, Renaud G, Cerato M *et al.* 2016. Tomography and imaging at the PSICHE beam line of the SOLEIL synchrotron. *Review of Scientific Instruments* 87: 093704.
- Klaus KV, Schulz C, Bauer DS, Stützel T. 2017. Historical biogeography of the ancient lycophte genus *Selaginella*: early adaptation to xeric habitats on Pangea. *Cladistics* 33: 469–480.
- Leroux O, Sørensen I, Marcus SE, Viane RLL, Willats WGT, Knox JP. 2015. Antibody-based screening of cell wall matrix glycans in ferns reveals taxon, tissue and cell-type specific distribution patterns. *BMC Plant Biology* 15: 56.
- Li S, Lens F, Espino S, Karimi Z, Klepsch M, Schenk HJ, Schmitt M, Schuldt B, Jansen S. 2016. Intervessel pit membrane thickness as a key determinant of embolism resistance in angiosperm xylem. *IAWA Journal* 37: 152–171.
- Lima TRA, Carvalho ECD, Martins FR, Oliveira RS, Miranda RS, Muller CS, Pereira L, Bittencourt PRL, Sobczak JCMSM, Gomes-Filho RCC *et al.* 2018. Lignin composition is related to xylem embolism resistance and leaf life span in trees in a tropical semiarid climate. *New Phytologist* 219: 1252–1262.
- Martin-StPaul N, Delzon S, Cochard H. 2017. Plant resistance to drought depends on timely stomatal closure. *Ecology Letters* 20: 1437–1447.
- McAdam SAM. 2015. Physicochemical quantification of abscisic acid levels in plant tissues with an added internal standard by ultra-performance liquid chromatography. *Bio-protocol* 5: 1–13.
- McAdam SAM, Brodribb TJ. 2012. Fern and lycophte guard cells do not respond to endogenous abscisic acid. *Plant Cell* 24: 1510–1521.
- McAdam SAM, Brodribb TJ. 2013. Ancestral stomatal control results in a canalization of fern and lycophte adaptation to drought. *New Phytologist* 198: 429–441.
- McElwain JC. 2011. Ferns: a xylem success story. *New Phytologist* 192: 307–310.
- McLean B, Juniper BE. 1979. The fine structure and development of the trabeculae and the trabecular ring in *Selaginella kraussiana*. *Planta* 145: 443–448.
- Mickel JT, Hellwig RL. 1969. Actino-plectostely, a complex new stelar pattern in *Selaginella*. *American Fern Journal* 59: 123–134.
- Mirone A, Brun E, Gouillart E, Tafforeau P, Kieffer J. 2014. The PyHST2 hybrid distributed code for high speed tomographic reconstruction with interaction reconstruction and a priori knowledge capabilities. *Nuclear Instruments and Methods in Physics Research Section B: Beam Interactions with Materials and Atoms* 324: 41–48.
- Motzer T, Munz N, Küppers M, Schmitt D, Anhu D. 2005. Stomatal conductance, transpiration and sap flow of tropical montane rainforest trees in southern Ecuadorian Andes. *Tree Physiology* 25: 1283–1293.
- Oliver MJ, Tuba Z, Brent DM. 2000. The evolution of vegetative desiccation tolerance in land plants. *Plant Ecology* 151: 85–100.
- Paganin D, Mayon SC, Gureyev TE, Miller PR, Wilkins SW. 2002. Simultaneous phase and amplitude extraction from a single defocused image of a homogeneous object. *Journal of Microscopy* 206: 33–40.
- Pampurova S, Van Dijk P. 2014. The desiccation tolerant secrets of *Selaginella lepidophylla*: What we have learned so far? *Plant Physiology and Biochemistry* 80: 285–290.
- Petrzell F, Pagliarani C, Savi T, Losso A, Cavalletto S, Tromba G, Dullin C, Bär A, Ganthaler A, Miotto A *et al.* 2018. The pitfalls of *in vivo* imaging techniques: evidence for cellular damage caused by synchrotron X-ray computed micro-tomography. *New Phytologist* 220: 104–110.
- Pittermann J, Limm E, Rico C, Christman MA. 2011. Structure–function constraints of tracheid-based xylem: a comparison of conifers and ferns. *New Phytologist* 192: 449–461.
- Powers JS, Vargas GG, Brodribb TJ, Schwartz NB, Pérez-Aviles D, Smith-Martin CM, Becknell JM, Aureli F, Blanco R, Calderón-Morales E *et al.* 2020. A catastrophic tropical drought kills hydraulically vulnerable tree species. *Global Change Biology* 26: 3122–3133.
- R Core Team. 2019. *mgcv: Mixed GAM computation vehicle with automatic smoothness estimation*, R v.1.8-31. Vienna, Austria: R Foundation for Statistical Computing [WWW document] URL <https://cran.r-project.org/web/packages/mgcv/index.html>.
- Rowe NP. 1988. A herbaceous lycophte from the Lower Carboniferous Drybrook Sandstone of the Forest of Dean, Gloucestershire. *Palaeontology* 31: 69–83.

- Ruszala EM, Beerling DJ, Franks PJ, Chater C, Casson SA, Gray JE, Hetherington AM. 2011. Land plants acquired active stomatal control early in their evolutionary history. *Current Biology* 21: 1030–1035.
- Sack L, Holbrook NM. 2006. Leaf hydraulics. *Annual Review of Plant Biology* 57: 361–381.
- Schmidt AR, Regalado L, Weststrand S, Korall P, Sadowski EM, Schneider H, Jansen E, Bechteler J, Krings M, Müller P *et al.* 2020. *Selaginella* was hyperdiverse already in the Cretaceous. *New Phytologist*. doi: 10.1111/nph.16600.
- Schneider EL, Carlquist S. 2000a. SEM studies on vessels of the homophyllous species of *Selaginella*. *International Journal of Plant Sciences* 161: 967–974.
- Schneider EL, Carlquist S. 2000b. SEM studies on the vessels of heterophyllous species of *Selaginella*. *International Journal of Plant Sciences* 127: 263–270.
- Schneider H, Schuettpehl E, Pryer KM, Cranfill R, Magallón S, Lupia R. 2004. Ferns diversified in the shadow of angiosperms. *Nature* 428: 553–557.
- Scholz A, Klepsch MM, Zohreh K, Jansen S. 2013. How to quantify conduits in wood? *Frontiers in Plant Science* 4: 56.
- Schulz C, Little DP, Stevenson DW, Bauer D, Moloney C, Stützel T. 2010. An overview of the morphology, anatomy, and life cycle of a new model species: the lycophyte *Selaginella apoda* (L.) spring. *International Journal of Plant Sciences* 171: 693–712.
- Schuster AC, Burghardt M, Riederer M. 2017. The ecophysiology of leaf cuticular transpiration: are cuticular water permeabilities adapted to ecological conditions? *Journal of Experimental Botany* 68: 5271–5279.
- Scoffoni C, Albuquerque C, Brodersen C, Townes SV, John GP, Bartlett MK, Buckley TN, McElrone AJ, Sack L. 2017. Outside-xylem vulnerability, not xylem embolism, controls leaf hydraulic decline during dehydration. *Plant Physiology* 173: 1197–1210.
- Soni DK, Ranjan S, Singh R, Khare PB, Pathre UV, Shirke PA. 2012. Photosynthetic characteristics and the response of stomata to environmental determinants and ABA in *Selaginella bryopteris*, a resurrection spike moss species. *Plant Science* 191–192: 43–52.
- Sterling C. 1970. Crystal-structure of ruthenium red and stereochemistry of its pectic stain. *American Journal of Botany* 57: 172–175.
- Stewart W, Rothwell G. 2010. *Paleobotany and the evolution of plants*. Cambridge, UK: Cambridge University Press.
- Trueba S, Pouteau R, Lens F, Feild TS, Isnard S, Olson ME, Delzon S. 2017. Vulnerability to xylem embolism as a major correlate of the environmental distribution of rain forest species on a tropical island. *Plant, Cell & Environment* 40: 277–289.
- Tyree MT, Hammel HT. 1972. The measurement of the turgor pressure and the water relations of plants by the pressure-bomb technique. *Journal of Experimental Botany* 23: 267–282.
- Tyree MT, Sperry JS. 1989. Vulnerability of xylem to cavitation and embolism. *Annual Review of Plant Physiology and Plant Molecular Biology* 40: 19–38.
- Urli M, Porté AJ, Cochard H, Guengant Y, Burlett R, Delzon S. 2013. Xylem embolism threshold for catastrophic hydraulic failure in angiosperm trees. *Tree Physiology* 33: 672–683.
- Ursache R, Andersen TG, Marhavý P, Geldner N. 2018. A protocol for combining fluorescent proteins with histological stains for diverse cell wall components. *The Plant Journal* 93: 399–412.
- van Doorn WG, Hiemstra T, Fanourakis D. 2011. Hydrogel regulation of xylem water flow: an alternative hypothesis. *Plant Physiology* 157: 1642–1649.
- Vanburen R, Wai CM, Ou S, Pardo J, Bryant D, Jiang N, Mockler TC, Edger P, Michael TP. 2018. Extreme haplotype variation in the desiccation-tolerant clubmoss *Selaginella lepidophylla*. *Nature Communications* 9: 13.
- Voragen AGJ, Coenen G-J, Verhoef RP, Schols HA. 2009. Pectin, a versatile polysaccharide present in plant cell walls. *Structural Chemistry* 20: 263.
- Weis KG, Polito VS, Labavitch JM. 1988. Microfluorometry of pectic materials in the dehiscence zone of almond (*Prunus dulcis* [Mill.] DA Webb) fruits. *Journal of Histochemistry and Cytochemistry* 36: 1037–1041.
- Weng J-K, Akiyama T, Bonawitz ND, Li X, Ralph J, Chapple C. 2010. Convergent evolution of syringyl lignin biosynthesis via distinct pathways in the lycophyte *Selaginella* and flowering plants. *Plant Cell* 22: 1033–1045.
- Weng J, Akiyama T, Ralph J, Chapple C. 2011. Independent recruitment of an O-methyltransferase for syringyl lignin biosynthesis in *Selaginella moellendorffii*. *Plant Cell* 23: 2708–2724.
- Weng J, Li X, Stout J, Chapple C. 2008. Independent origins of syringyl lignin in vascular plants. *Proceedings of the National Academy of Sciences, USA* 105: 7887–7892.
- Zhang Y, Carmesin C, Kaack L, Klepsch MM, Kotowska M, Matei T, Schenk HJ, Weber M, Walther P, Schmidt V *et al.* 2020. High porosity with tiny pore constrictions and unbending pathways characterise the 3D structure of intervessel pit membranes in angiosperm xylem. *Plant, Cell & Environment* 43: 116–130.
- Zhang Y, Klepsch MM, Jansen S. 2017. Bordered pits in xylem of vesselless angiosperms and their possible misinterpretation as perforation plates. *Plant, Cell & Environment* 40: 2133–2146.
- Zhou XM, Rothfels CJ, Zhang L, He ZR, Le Pêchon T, He H, Lu NT, Knapp R, Lorence D, He XJ *et al.* 2016. A large-scale phylogeny of the lycophyte genus *Selaginella* (Selaginellaceae: Lycopodiopsida) based on plastid and nuclear loci. *Cladistics* 32: 360–389.
- Ziegler C, Coste S, Stahl C, Delzon S, Levionnois S, Cazal J, Cochard H, Esquivel-Muelbert A, Goret J-Y, Heuret P *et al.* 2019. Large hydraulic safety margins protect Neotropical canopy rainforest tree species against hydraulic failure during drought. *Annals of Forest Science* 76: 115.

Supporting Information

Additional Supporting Information may be found online in the Supporting Information section at the end of the article.

Fig. S1 Light microscopy image of the stele in a transverse stem section of *Selaginella pulcherrima*.

Fig. S2 Micro-CT scans before and after rehydration.

Table S1 Equations for relationships.

Please note: Wiley Blackwell are not responsible for the content or functionality of any Supporting Information supplied by the authors. Any queries (other than missing material) should be directed to the *New Phytologist* Central Office.